

# The Impact and Spreading of Ink Jet Printed Droplets

Jonathan Stringer and Brian Derby; School of Materials, University of Manchester; Manchester, United Kingdom

## Abstract

*Ink jet printing is a fabrication technique that shows potential for use in fields such as printed electronics, biomaterials and MEMS. The attainable feature size and spacing of a component manufactured in this fashion is determined by the generated droplet size, how the droplets interact with the substrate and how adjacent droplets interact with each other. An individual droplet of material-laden ink will form a deposit with a diameter dependent upon the generated droplet size and the contact angle formed between the droplet and the substrate. This diameter can be accurately predicted using a spherical cap assumption and macroscopic contact angle data. As droplets are moved closer together on a substrate, they appear to interact with each other at distances greater than the predicted equilibrium diameter of a droplet. The amount of interaction between droplets increases with decreasing equilibrium contact angle. This interaction could either be due to changes in the local vapour pressure around previously deposited droplets or impact-driven spreading of the droplet beyond the equilibrium state.*

## Introduction

Ink jet printing is a non-contact, additive technique for fabricating structures from material-laden inks, with applications in printed electronics [1], biomaterials [2] and MEMS [3]. The technique works by selectively ejecting a small (~1-1000 pl) droplet towards a substrate; this droplet will spread upon impact with the substrate, coalesce with any adjacent droplets and change phase to form a solid deposit. Understanding the spreading, coalescence and phase change experienced by deposited droplets is crucial, as it determines the feature resolution and spacing attainable with ink jet printing.

The deposition of a single droplet can be divided into two stages: a stage driven by the impact kinetic energy that proceeds until this energy is dissipated, and a surface energy driven stage where the droplet will spread to a diameter dependent upon the surface energy interactions between the droplet and the substrate. Both of these stages can control the deposit size, with a 'fast' phase change (e.g. solidification [4]) being controlled by the impact-driven stage and a 'slow' phase change (e.g. evaporation) being controlled by the surface energy driven stage.

If gravitational forces are negligible, a liquid droplet will come to rest on a substrate as a spherical cap with a contact angle,  $\theta$ . The extent of droplet spreading upon the substrate due to surface energy as a function of  $\theta$  can be calculated:

$$\beta_{eqm} = d_{eqm}/d = 2(\tan(\theta/2)(3 + \tan^2(\theta/2)))^{-1/3} \quad (1)$$

where  $\beta_{eqm}$  is the ratio of the initial droplet diameter,  $d$ , to the diameter of the droplet on the substrate,  $d_{eqm}$ . Droplets loaded

with material often show a contact angle hysteresis due to the solid phase segregating to the contact line upon evaporation and pinning it [5]. The result of this is that the area of substrate covered by a solid deposit will be the same as the area covered by liquid precursor. When droplets are printed such that their footprints overlap, the droplets will coalesce to form beads [6].

The morphology of the formed beads changes as the inter-droplet spacing,  $p$ , is changed and can be separated into three regions. Region 1 consists of a series of bulges connected by ridges of width  $\beta_{eqm}d$ . This has been explained in terms of two competing flows within the bead; the flow into the bead due to the speed of droplet deposition and axial flow driven by pressure differences inherent within the bead [6]. When the flow into the bead is exceeded by the axial flow, then liquid flows down the bead to the area of lower pressure rather than outward due to capillarity. The occurrence of this morphology is dependent upon both fluid and machine parameters, in addition to  $p$ ,  $d$  and  $\theta$ . The threshold value of  $p$  when this instability is no longer formed ( $p_{1-2}$ ) is difficult to define analytically due to the complex nature of the flow. In general, it is found that  $p_{1-2}$  is reduced as  $\theta$  and ink viscosity are reduced, and surface tension and speed of droplet deposition is increased.

Region 2 occurs when  $p_{1-2} < p < p_{2-3}$ , with a morphology consisting of beads of variable width with parallel contact lines. The width,  $w$ , of a liquid bead in this region can be calculated as a function of  $p$ ,  $\theta$  and  $d$  by assuming the bead has a truncated circle cross section and that volume is conserved:

$$w = (2\pi d^3/[3p(\theta/\sin^2\theta - \cos\theta/\sin\theta)])^{0.5} \quad (2)$$

Region 3 occurs when  $p_{2-3} < p < \beta_{eqm}d$ , and is due to the volume of liquid not being sufficient to form a bead with parallel contact lines of width equal to  $\beta_{eqm}d$ , a limit introduced by the presence of contact line pinning. The morphology of region 3 consists of a wavy contact line with the maximum bead width being equal to  $\beta_{eqm}d$ , where the point of maximum bead width is separated by a distance equal to  $p$ . The value of  $p_{2-3}$  can be calculated using the same truncated circle assumption as used for equation 2:

$$p_{2-3} = 2\pi d/[3\beta_{eqm}^2(\theta/\sin^2\theta - \cos\theta/\sin\theta)] \quad (3)$$

If there is no interaction between neighbouring droplets, the deposits formed when  $p > \beta_{eqm}d$  should consist of a series of discrete droplets of diameter  $\beta_{eqm}d$ . Any interaction between adjacent droplets could lead to a change in the deposit morphology, which would have consequences for the spacing of droplets. This could be critical when designing components where their successful function could be jeopardized by any overlapping of neighbouring deposits, such as in printed electronics.

## Experimental Procedure

The ink used in this study was an organometallic salt dissolved in xylene synthesised in-house, preparation details for which have been published previously [7]. The substrates used in this study were glass (microscope slides, BDH, Poole, Dorset, UK), polyimide film (Kapton™, DuPont, Wilmington, DE, USA) and silicone rubber (Goodfellow Cambridge Ltd., Huntingdon, Cambs., UK). The equilibrium contact angle,  $\theta$ , of each ink/substrate combination was measured using a CCD camera and image analysis software (FTA 200, Camtel, Royston, UK).

Printing of samples was carried out using a JetLab printing platform (MicroFab Inc., Plano, TX, USA) that consists of a piezoelectric squeeze mode print head situated above a programmable x-y platform. The print heads used in this study had a nozzle diameter of 60  $\mu\text{m}$  (MJ-AB-01-60, MicroFab, as above). Droplet diameter measurements were conducted by weighing a known number of ejected droplets and calculating the droplet diameter, assuming a spherical droplet and known density values. All substrates were cleaned with acetone before deposition of droplets. A constant droplet generation frequency of 1 kHz was used for all samples to eliminate any variation in droplet size and velocity due to acoustic resonance. Samples were printed with varying  $p$  and the formed deposit analysed using optical microscopy.

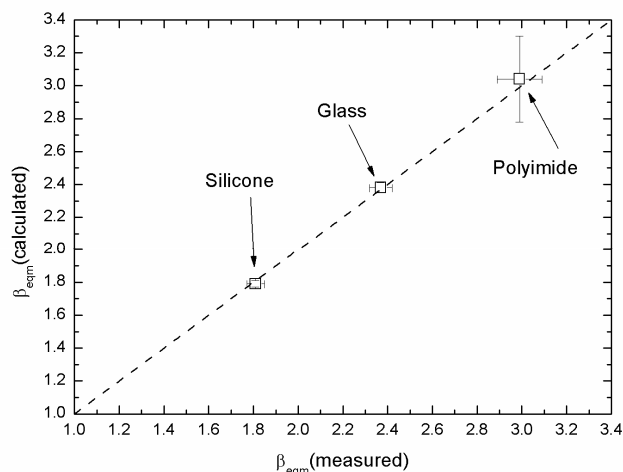


**Figure 1** Calculated  $\beta_{eqm}$  compared with measured  $\beta_{eqm}$  for a variety of substrates with different values of  $\theta$ . For silicone,  $\theta = 47^\circ$ , for glass,  $\theta = 22^\circ$ , for polyimide,  $\theta = 10.8^\circ$ .

## Results and Discussion

The size of an individual generated droplet was measured using the method described above and it was found that  $d = 65 \mu\text{m}$ , slightly larger than the nozzle diameter. The diameter of deposit left by a single droplet ( $d_{eqm}$ ) was measured for each substrate used and the extent of spreading,  $\beta_{eqm}$ , compared with the value of  $\beta_{eqm}$  calculated with equation 1, using values of  $\theta$  obtained experimentally. As shown in Figure 1, there is good agreement between measured and calculated values for all substrates. This indicated that gravitational effects are negligible, as would be

expected at this length scale, and that contact line pinning takes place due to segregation of precipitated salt to the contact line.

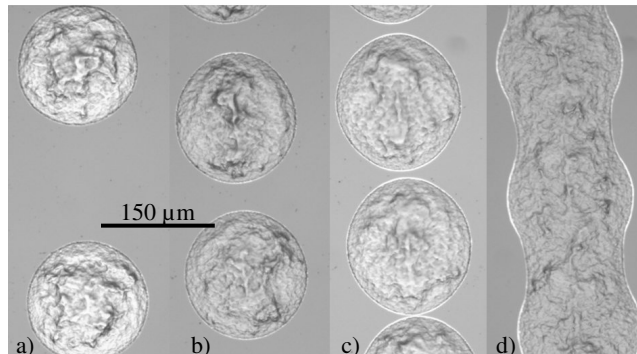


**Figure 2** A typical series of deposits formed from droplets of organometallic ink deposited on glass. a)  $p = 280 \mu\text{m}$ , b)  $p = 200 \mu\text{m}$  c)  $p = 180 \mu\text{m}$  d)  $p = 170 \mu\text{m}$ .  $\beta_{eqm}d = 156 \mu\text{m}$  in all cases.

To investigate the interaction of adjacent droplets, lines of droplets were printed with a known droplet spacing,  $p$ . When  $p$  was much greater than  $\beta_{eqm}d$ , there were no signs of interaction between droplets, with a series of deposits identical to a single droplet being formed (Figure 2a). As  $p$  is reduced towards  $\beta_{eqm}d$  the deposit morphology begins to change, with drops becoming elongated in the direction of droplet deposition (Figure 2b). This elongation becomes greater with reducing  $p$  until neighbouring deposits come into contact with each other and form a single linear deposit (Figure 2c-d). This occurred while  $p$  was still greater than  $\beta_{eqm}d$ .

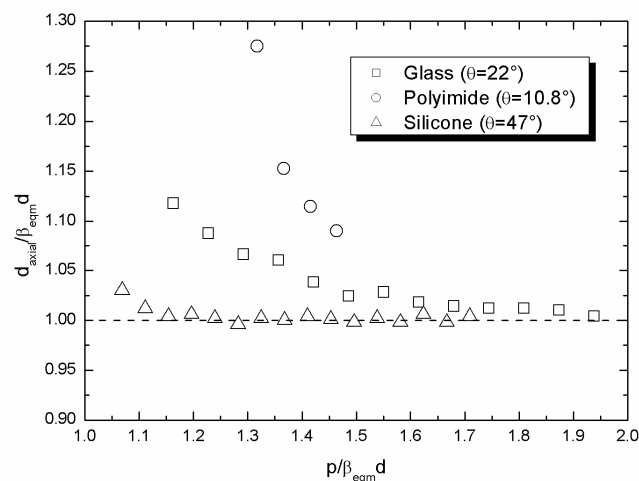


**Figure 3** Normalised  $d_{axial}$  against normalised  $p$  for all 3 substrates

The influence of  $\theta$  on this interaction was investigated by printing as before but on 3 different substrates. The degree of interaction between adjacent droplets was quantified by measuring the diameter of the deposit in the direction of droplet deposition ( $d_{axial}$ ). The variation of  $d_{axial}$  with  $p$  was normalized with respect to  $\beta_{eqm}d$  and plotted (figure 3). Figure 3 shows that the interaction increased as  $\theta$  decreased and that the normalized value of  $p$  at

which discrete deposits are observed increases with decreasing  $\theta$ . These variations with  $\theta$  show that the degree of interaction, and the distance over which this interaction takes place, increases as the contact angle decreases.

The nature of the interaction between adjacent droplets is not immediately apparent from current results. The interaction will either be due to a change in the deposition environment caused by previously deposited droplets, or due to direct contact between droplets.

The time between droplet depositions is given by the inverse of the frequency and found to be 1 ms. After this length of time, it is likely that a droplet will still be evaporating and producing solvent vapour into the immediate surroundings. If the volume into which this evaporation takes place coincides with the location of the next droplet, the increased vapour pressure could affect the surface energy equilibrium and change  $\theta$ . To evaluate what influence vapour pressure may have on  $\theta$ , deposits were made of  $d=2\text{mm}$  droplets both in ambient conditions and in a chamber saturated with solvent vapour. It was found that the diameter of deposit increased significantly when produced in a saturated environment, with the increase being greatest for polyimide and glass.

A droplet impacting a solid surface will initially spread to dissipate the impact kinetic energy it possesses. The maximum diameter reached by the droplet upon impact will depend upon the amount of kinetic energy and the route of viscous dissipation within the droplet, in addition to any surface energy considerations. Models previously derived for the spreading of large (mm-size) droplets indicate that droplets will not spread beyond  $\beta_{eqm}d$  under typically encountered ink jet printed conditions. Previous studies of the impact of ink jet droplets [8] have shown that these models tend to under-predict at low impact velocities and over-predict at high impact velocities. This suggests that the impact-driven spreading of ink jet droplets may be more surface energy controlled than for larger droplets. The nature of the droplet interaction could therefore be that an impacting droplet will extend beyond  $\beta_{eqm}d$  and make contact with a neighbouring droplet before recoiling towards equilibrium, pulling the pre-deposited droplet out of equilibrium.

## Conclusion

Individual droplets of an organometallic salt solution deposited by ink jet printing were found to form deposits with a diameter controlled by contact angle and generated droplet size. Droplets positioned at spacing greater than this diameter were still found to interact, with this interaction increasing with decreasing contact angle. The nature of this interaction was not apparent from obtained results, but it was postulated to be either due to an increased local vapour pressure or by droplet spreading beyond equilibrium upon impact.

## Acknowledgements

This work was funded by the Office of Naval Research through grant N00014-03-1-0930.

## References

1. Sirringhaus, H., et. al., 'High-resolution inkjet printing of all-polymer transistor circuits', *Science*, 2000, 290(5499), 2123-2126.
2. Sachlos, E., et. al., 'Novel collagen scaffolds with predefined internal morphology made by solid freeform fabrication', *Biomaterials*, 2003, 24(8), 1487-1497.
3. Fuller, S.B., et. al., 'Ink-jet printed nanoparticle microelectromechanical systems', *J. MEMS.*, 2002, 11(1), 54-60.
4. Schiaffino, S., and Sonin, A.A. 'Formation and stability of liquid and molten beads on a solid surface', *J. Fluid Mech.*, 1997, 343, 95-110.
5. Deegan, R.D., et. al. 'Contact line deposits in an evaporating drop', *Phys. Rev. E.*, 2000, 62(1), 756-765.
6. Duineveld, P.C. The stability of ink-jet printed lines of a liquid with zero receding contact angle on a homogeneous substrate. *J. Fluid Mech.*, 2003, 477, 175-200.
7. Dearden, A.L., et. al. A low curing temperature silver ink for use in ink-jet printing and subsequent production of conductive tracks. *Macromol. Rapid Commun.*, 2005, 26, 315-318.
8. Van Dam, D.B. and Le Clerc, C., 'Experimental study of the impact of an ink-jet printed droplet on a solid substrate', *Phys. Fluids*, 2004, 16(9), 3403-3414

## Biography

*Jonathan Stringer is currently in the final year of his PhD in the School of Materials at the University of Manchester, United Kingdom. He was previously awarded an MEng in Materials Science, also from the University of Manchester. His research looks into the physics of ink jet printing, in particular the processes of droplet deposition, coalescence and phase change from printable ink to functional material.*